



Supplement of

Assessing sensitivities of climate model weighting to multiple methods, variables, and domains in the south-central United States

Adrienne M. Wootten et al.

Correspondence to: Adrienne M. Wootten (amwootte@ou.edu)

The copyright of individual parts of the supplement might differ from the article licence.

S.1 Equations for Weighting Schemes

This section contains the equations for each of the four weighting schemes used in this study. Many of these weighting schemes are drawn from prior literature. As such, they are summarized in the manuscript text, Section 2.4, but the details of the equations are included here. We refer the authors to the prior literature where appropriate for some of the weighting schemes and equations.

S.1.1. Historical Skill and Historical Independence Weighting (SI-h)

The Historical Skill and Historical Independence Weighting (SI-h here and in the main text) is described in full by Sanderson et al. (2017). For full details we refer the reader to Sanderson et al. (2017) and the process and weighting is described here in brief. The SI-h uses a normalized area-weighted root mean square error (RMSE) matrix. This matrix compares the RMSE of each model against the observations (representing the skill) and each model against all other models (representing the independence). Sanderson et al. (2017) uses a normalized matrix for each variable to linearly combine and produce one set of weights. Since this study focused on singular variables independently, and not on a multivariate weighting, we used a single normalized RMSE matrix calculated separately for pr (annual total precipitation) and tasmx (annual average of daily high temperature). As described in Section 2, the weights for each variable are calculated separately.

The normalized area weighted RMSE matrix over the domain is used to calculate separate weights for skill and independence. The independence weights are calculated by first computing a similarity score from the RMSE matrix:

$$S(\delta_{ij}) = e^{-\left(\frac{\delta_{ij}}{D_u}\right)^2} \quad (S1)$$

Where S is the similarity score, δ_{ij} is the RMSE between models i and j , and D_u is the radius of similarity. The radius of similarity (Sanderson et al. 2015) is a free parameter that determines the distance over which models are considered similar and are downweighted for co-dependence. For simplicity, we retained the same value for D_u used by Sanderson et al. (2017), $D_u = 0.48$. Given the similarity score for a model i , the effective repetition is calculated as:

$$R_u(i) = 1 + \sum_{j \neq i}^n S(\delta_{ij}) \quad (S2)$$

Where $R_u(i)$ is the effective repetition of model i , and n is the total number of models. The independence weight, w_u , for model i is the inverse of its effective repetition:

$$w_u(i) = (R_u(i))^{-1} \quad (S3)$$

40 The skill weights are also calculated based on the normalized RMSE matrix, specifically, the
 41 normalized RMSE of each model against the observations. The skill weight, w_q , for model i is
 42 calculated as:

$$w_q(i) = e^{-\left(\frac{\delta_{i(obs)}}{D_q}\right)^2} \quad (S4)$$

43 Where D_q is the radius of model quality, set to 0.8 to match Sanderson et al. (2017). Finally, the overall
 44 weight, w , for model i is calculated as:

$$w(i) = Aw_u(i)w_q(i) \quad (S5)$$

45 Where A is a normalization constant such that the overall weights of all models sum to one.
 50

51 **S.1.2. Historical Skill and Future Independence Weighting (SI-c)**

52 One can argue that downscaling nudges every model toward the historical observations during the
 53 historical period because of the bias correction in the statistical downscaling process. As such, one
 54 would expect the historical skill of a downscaled ensemble to be high and the independence to be low.
 55 The Historical Skill and Future Independence Weighting (SI-c here and in the main text) was designed
 56 by Wootten et al. (2020) to account for this feature of statistical downscaling. The SI-c follows the same
 57 calculations as the SI-h. However, where the SI-h uses the normalized RMSE matrix of each model
 58 against all models in the historical period to calculate independence weights, the SI-c uses a normalized
 59 RMSE matrix of the projected change signal of each model against the other. That is, the independence
 60 weighting in the *SI-c focuses on the repetition of the change signal* while the *SI-h focuses on the
 61 repetition of the historical climatology*. This is a key difference between the SI-h and SI-c, but the
 62 equations are themselves identical between both weighting schemes

63 **S.1.3. Historical Skill Weighting (Skill)**

64 Weighting an ensemble for skill is one of the most well-known approaches to multi-model ensemble
 65 weighting. This study makes uses of the normalized area-weighted root mean square error (RMSE)
 66 between each model and the observations for the skill weighting. The Skill weighting scheme used here
 67 is in essence only the skill component of weighting from Sanderson et al. (2015; 2017) also described in
 70 Section S.1.1. After calculating the skill weight for each model i , the weights are normalized in the
 71 following manner:

$$w(i) = \frac{w(i)}{\sum_{i=1}^n w(i)} \quad (S6)$$

75 Where n is the number of models.

S.1.4. Bayesian Model Averaging

80 Bayesian Model Averaging (BMA) is different from other model averaging methods because it explicitly estimates each model's weight and its uncertainty by maximizing a likelihood function that represents the fit to the historical observations. In other words, BMA provides model weights that produce model combinations with the maximum likelihood of matching the observed data compared to other model combinations. In this study, using the optimized weights, BMA constructs the mean and uncertainty distribution of the climate metric of interest.

85 Since the BMA method estimates a distribution of model weights, various model combinations become possible, which provides a solution to the model dependence issue. In other words, consider that in the BMA framework there is a hypothetical Model A and a Model B that are similar and therefore not independent. Model A may have higher weights in some combinations, and conversely, Model B might
90 have higher weights in other combinations. Consequently, if both models are rewarded in the same set of weights, it is very likely that each model receives a reduced weight since both models are providing information to the model average. See Supplementary Section 2 of Massoud et al., (2020a) for additional details on how dependence is inferred with the BMA method.

95 The estimated model weights using BMA are as follows:

$$w_{m,BMA} = [w(m_1), w(m_2), \dots, w(m_k)] \quad (S7)$$

100 where $w(m_i, i = 1, 2, 3, \dots, k)$ represents the optimized weights of K models after fitting the observations using the likelihood function. The range of $w(m_i)$ is between 0 and 1, with a weight of 0 for models that do not contribute any information and a weight of 1 for models that fully contribute to the projection. The sum of a given combination of model weights is equal to 1. The final estimates of the BMA model weights, or $w_{m,BMA}$ in Eq. (S7), are utilized to constrain the spread of uncertainty in the projected end of century climate.

105

Our likelihood function is set up here as:

$$L(w_{m,BMA}) = -\frac{1}{2} \sum_{i,j} [Y_{ij} - X_{ij}(w_{m,BMA})]^2 \quad (S8)$$

110 where i, j refers to the longitudinal and latitudinal indices of grids on the map; $Y(i, j)$ is the observed climate metric at grid i, j ; and $X(i, j)$ is the BMA-weighted model ensemble average of the climate metric at grid i, j . We apply heavy sampling on the

possible model weight combination in search of model weights that maximize the likelihood function in Eq. (S7), which allows for the estimation of the optimized model weights, or $w_{m,BMA}$ in Eq. (S8).

S.2 Maps from the CMIP5 ensembles - precipitation

115 Among the 288 ensemble means created from this experimental setup, there are numerous times when
results are duplicated. For example, applying a given weighting combination created using the full
domain to Louisiana would have the same value as the same weighting combination created using the
full domain applied to the full domain and examining only the Louisiana area. As such, the results in
this and the following sections will focus only on those ensemble means created from the various
120 combinations of weighting schemes applied to the full domain for each ensemble. In this way, one can
then examine the effects for the Louisiana and New Mexico domains and other regions of the full
domain.

The bias for the CMIP5 ensemble means of precipitation are shown in Figure 8, and they depict the
125 influence of the different weighting schemes. For reference, the precipitation bias of the unweighted
ensemble mean shows a tendency to overestimate precipitation in the western portion of the domain and
underestimate in the eastern portion of the full domain (Figure 8, larger map on the left). For those
ensemble means created with temperature-derived weights (Figure 8, group of maps in the top right),
the pattern of bias in precipitation remains consistent but changes in magnitude compared to the
130 unweighted scheme. When weighted for the full domain (Figure 8, group of maps in the top right, top
row of figures), the bias pattern of precipitation is similar. When weighted for high temperatures in
Louisiana (Figure 8, group of maps in the top right, middle row of figures), the magnitude of
underestimation of precipitation in the eastern portion of the domain is smaller. In contrast, when
weighted for high temperatures in New Mexico (Figure 8, group of maps in the top right, bottom row of
135 figures), precipitation is underestimated by a larger amount in the eastern portion of the domain
compared to the full domain temperature weighting. When precipitation is used to derive the weights
(Figure 8, group of maps in the bottom right), the resulting ensemble mean of precipitation is sensitive
to the domain used for the weighting. When the full domain precipitation is used for weighting (Figure
8, group of maps in the bottom right, top row of figures), the ensemble mean shows a consistent pattern
140 to the bias of the unweighted ensemble mean. Additionally, the magnitudes of the bias in the full
domain are decreased using the BMA weighting scheme, which agrees with the results from Wooten et
al. (2020a). When weighted for precipitation in Louisiana (Figure 8, group of maps in the bottom right,
middle row of figures), the precipitation bias of the ensemble mean is overestimated across much of the
larger domain with a lower bias in Louisiana. In contrast, when weighted for precipitation in New
145 Mexico (Figure 8, group of maps in the bottom right, bottom row of figures), the precipitation bias of
the ensemble mean is underestimated across much of the larger domain, particularly in the eastern
portion of the domain and when using the BMA weighting.

The future projected change maps of precipitation for the CMIP5 ensemble, shown in Figure 9, are also
150 sensitive to the weighting combination used. The unweighted CMIP5 ensemble mean (Figure 9, larger

map on the left) projects a decrease in precipitation across much of Texas and New Mexico, with increases in precipitation projected in the northeast portion of the domain. When weighted for high temperature in the full domain (Figure 9, group of maps in the top right, top row of figures), the pattern remains consistent for each ensemble mean, with an expansion of projected decreases into the northern portion of the domain with the BMA weighting. The area of projected decreases shrinks for three out of four weighting schemes (all schemes except the BMA method) when high temperatures in Louisiana are used to derive the weights (Figure 9, group of maps in the top right, middle row of figures). Using BMA and Louisiana high temperatures to derive the ensemble weighting, the ensemble mean has a similar pattern and magnitude to the ensemble mean created with BMA weights derived using high temperatures in the full domain. In contrast, using New Mexico's high temperatures to derive ensemble weights (Figure 9, group of maps in the top right, bottom row of figures) causes the area of projected decreases in the ensemble mean to shrink to a region along the Gulf Coast, with projected increases in the northeast and northwest corners. Using precipitation in the full domain to derive ensemble weights (Figure 9, group of maps in the bottom right, top row of figures), three of the four weighting schemes have a similar pattern to the unweighted mean, while the BMA weighted ensemble mean has a much weaker drying signal and a large increase in precipitation in the northeast corner of the domain. The greatest contrast between the CMIP5 ensemble means exists between the means created with weights based on Louisiana and New Mexico precipitation (Figure 9, group of maps in the bottom right, middle, and bottom row of figures). When Louisiana precipitation is used to derive ensemble weights (Figure 9, group of maps in the bottom right, middle row of figures), the ensemble mean shows an increase in precipitation across the eastern portion of the domain. The greatest increase in precipitation is in the northeast corner of the domain for three of four weighting schemes, while the greatest increase in the ensemble mean using the BMA weighting derived with Louisiana precipitation is actually in Louisiana. The ensemble mean created with weights derived from New Mexico precipitation (Figure 9, group of maps in the bottom right, bottom row of figures) projects a decrease in precipitation across New Mexico, much of Texas, and all of Louisiana with three out of four weighting schemes. When BMA weights are derived using New Mexico precipitation, the resulting ensemble mean projects a decrease in precipitation across the entire domain, with the greatest magnitude along the Gulf Coast.

S.3 Maps from CMIP5 ensembles – high temperature

There is more consistency in the historical bias and future projected changes of the weighted CMIP5 ensembles of high temperatures, shown in Figure 10, compared to that of precipitation, and these weighted ensembles are less sensitive to the various weighting combinations. The bias of the unweighted CMIP5 ensemble mean high temperature (Figure 10, larger map on the left) shows a tendency to underestimate high temperatures in the western portion of the domain except for some mountainous regions where the bias is variable. When weights are derived using high temperatures in either the full domain or Louisiana (Figure 10, group of maps in the top right, top, and middle row of figures), the pattern remains similar to the unweighted mean regardless of the weighting scheme used. The ensemble means tend to overestimate temperatures east of the Rocky Mountains when the ensemble weights are derived using New Mexico high temperatures (Figure 10, group of maps in the top right, bottom row of figures). When using precipitation in the full domain to derive the ensemble

weights (Figure 10, group of maps in the bottom right, top row of figures), the bias for the resulting ensemble means is similar to the unweighted mean, but the high temperature is broadly underestimated when Louisiana precipitation is used to derive ensemble weights (Figure 10, group of maps in the bottom right, middle row of figures). In contrast, when New Mexico precipitation is used to derive ensemble weights (Figure 10, group of maps in the bottom right, bottom row of figures), high temperatures east of the Rocky Mountains are overestimated, particularly in the northeastern portion of the region. However, the magnitude of the overestimate is not as large as the overestimate of high temperatures when the New Mexico high temperatures are used to derive ensemble weights.

As with the high temperature bias, Figure 11 shows that the future projected changes in high temperature in the resulting ensemble means are less sensitive than projected changes in precipitation with the CMIP5 ensemble (i.e., plots in Figure 9). If the full domain precipitation (Figure 11, group of maps in the bottom right, top row of figures) or high temperature (Figure 11, group of maps in the top right, top row of figures) are used to derive the ensemble weights, the ensemble mean change from three out of four weighting schemes tends to have a similar pattern to the unweighted ensemble mean. The weighting with BMA using the full domain high temperatures results in a similar pattern of projected changes in high temperature but concentrates the greatest changes in the northern portion of the domain. Similarly, the weighting with BMA using the full domain precipitation results in a similar pattern of projected changes in high temperature but concentrates the greatest changes on the western edge of the domain. The projected changes in high temperature are larger, particularly in the northwest corner of the domain with BMA, when New Mexico high temperatures (Figure 11, group of maps in the top right, bottom row of figures) or precipitation (Figure 11, group of maps in the bottom right, bottom row of figures) are used to derive ensemble weights. The greatest projected changes in high temperature are in the ensemble mean when created using weights derived with New Mexico precipitation and the BMA weighting scheme. With regards to the Louisiana domain (Figure 11, group of maps in the bottom right, middle row of figures), there is a notable difference in the projected change in high temperature. When the high temperatures in Louisiana are used to derive ensemble weights, the projected high temperature changes follow a similar pattern to the unweighted ensemble mean, however, the projected high temperature changes are less than the unweighted mean and the other ensemble means.

S.4 Maps from the LOCA ensembles – precipitation and high temperature

Previous work by Wootten et al. (2020a) has shown that the future projected changes from a resulting ensemble mean can be sensitive to whether or not downscaling was used in the ensemble. In addition, downscaling also reduces the bias of the individual members of a GCM. The bias reduction resulting from the LOCA downscaling of precipitation projections is demonstrated by the comparison between Figure S1 to Figure 8. The bias reduction resulting from the LOCA downscaling of high temperature projections is demonstrated by the comparison between Figure S2 to Figure 10. For both variables, the use of downscaling demonstrably reduces the bias of the ensemble across all three domains (Figures S3-S6). As such, the results in this section will focus on the projected changes of high temperature and precipitation using the downscaled LOCA ensemble.

The precipitation future projected change from the unweighted mean for the LOCA ensemble is shown in Figure 12 (larger map on the left) and displays a similar pattern to the unweighted CMIP5 ensemble (from Figure 9), with a decrease in precipitation projected along the Gulf Coast and a projected increase in the northeast corner of the domain. When weighting is based on high temperature in all three
235 domains (Figure 12, group of maps in the top right), the projected change in precipitation is similar to the unweighted ensemble mean (with some changes in magnitude) for all of the weighting schemes except for BMA. When weighting is based on the full domain and Louisiana high temperatures with the BMA weighting scheme, the LOCA ensemble mean projects an increase in precipitation across much of the eastern and northern portions of the domain, and any area showing a projected decrease is confined
240 to southern Texas. When weighting is derived using New Mexico high temperatures and the BMA weighting scheme, the same region of southern Texas is projected to see decreases in precipitation as the unweighted version and with a larger magnitude. However, when looking at this scheme, the projected increases in rainfall are primarily in the northern area of the domain with lesser magnitude than other BMA weighted means weighted based on high temperature. When using the full domain
245 precipitation to derive ensemble weights (Figure 12, group of maps in the bottom right), the resulting ensemble mean precipitation changes are similar to the unweighted precipitation change, though the BMA weighted version also includes a greater increase in precipitation in the northwest corner of the domain. When weighted on precipitation in New Mexico or Louisiana with the LOCA ensemble (Figure 12, group of maps in the bottom right, middle, and bottom row of figures), the ensemble means for three
250 of the four weighting schemes have a similar projected change to the unweighted ensemble mean. When the ensemble weights are derived using Louisiana precipitation with the BMA weighting scheme, the resulting LOCA ensemble mean projects an increase in precipitation in the eastern portion of the domain, with little to no change in other parts of the domain. The BMA weighted mean of the LOCA ensemble projects a decrease in precipitation along the Gulf Coast and Louisiana and an increase across
255 much of the rest of the domain when New Mexico precipitation is used to derive weights.

The unweighted mean high temperature change for the LOCA ensemble, shown in Figure 13 (larger map on the left) is similar to the CMIP5 ensemble (from Figure 11). For three out of four weighting schemes (all schemes except BMA), the resulting ensemble mean projected change for high temperature
260 tends to be similar to that of the unweighted ensemble mean. However, the resulting LOCA ensemble mean created with the BMA weighting is sensitive to the domain and variable used to derive weights. When the full domain or Louisiana high temperatures are used with BMA to derive model weights (Figure 12, group of maps in the top right), the mean projected high temperature changes are demonstrably cooler across the entire domain, particularly in the northwest corner of the domain. When
265 New Mexico high temperatures are used to derive the BMA weights, the gradient of the projected change remains consistent except for a cool pocket in southern Colorado and northern New Mexico. In contrast, when the full domain or New Mexico precipitation are used with BMA to derive ensemble weights for the LOCA ensemble (Figure 13, group of maps in the bottom right), the projected changes in high temperature are warmer than the unweighted mean, particularly in the northwest corner of the
270 domain. However, when Louisiana precipitation is used to derive ensemble weights with BMA, the mean change from the LOCA ensemble is cooler than the unweighted mean for much of the domain.

275

280

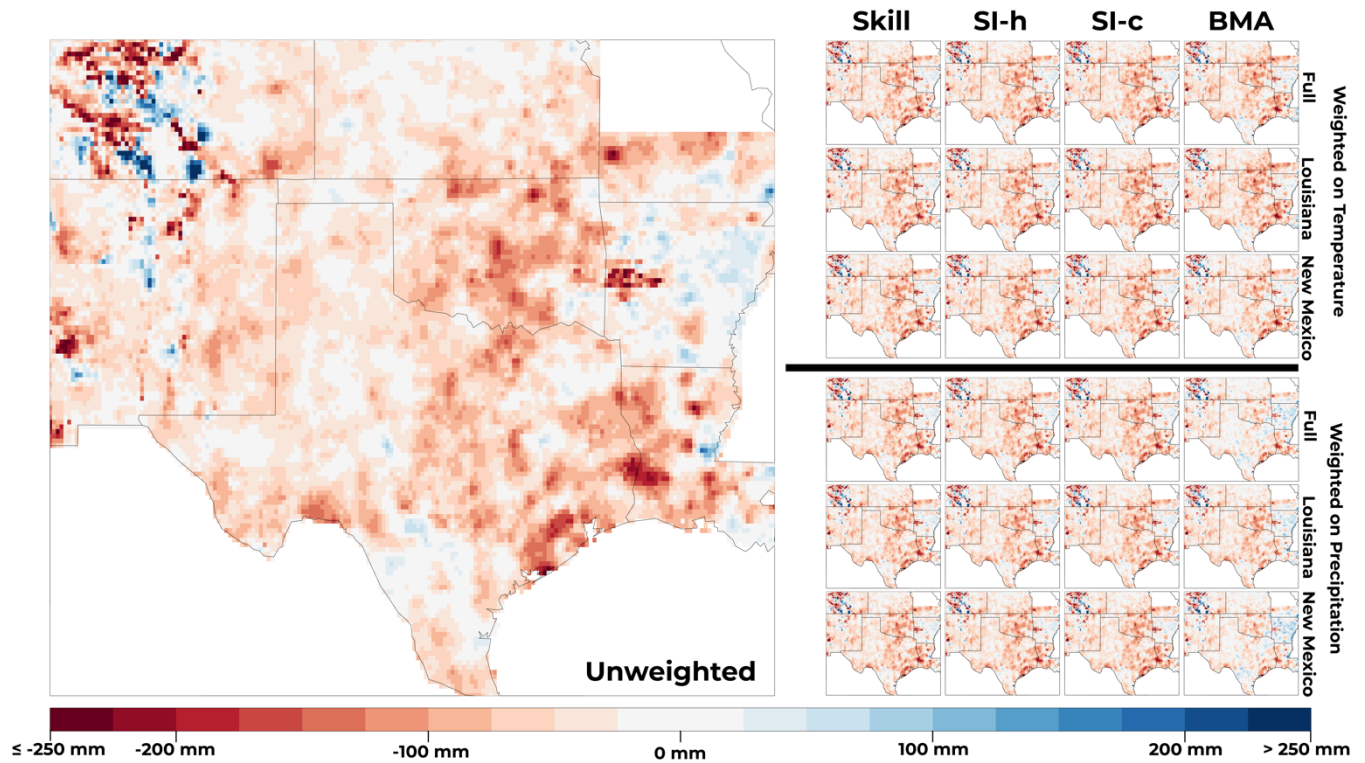
285

290

295

300

Supplemental Tables and Figures



305 Figure S1: Bias of LOCA ensemble mean precipitation (1981-2005) from the unweighted ensemble (left) and each weighted
 ensemble mean (right). On the right side, the columns from left to right are for the Skill, SI-h, SI-c, and BMA weighting schemes
 respectively. On the right side, the top group of twelve plots are the results for weights derived using temperature (tmax) and the
 bottom group of twelve plots are the results for weights derived using precipitation (pr). Within a group of twelve on the right-
 hand side, the top row is for weights deriving using the full domain, the middle row is for weights derived using the Louisiana
 310 domain, and the bottom row is for weights derived using the New Mexico domain.

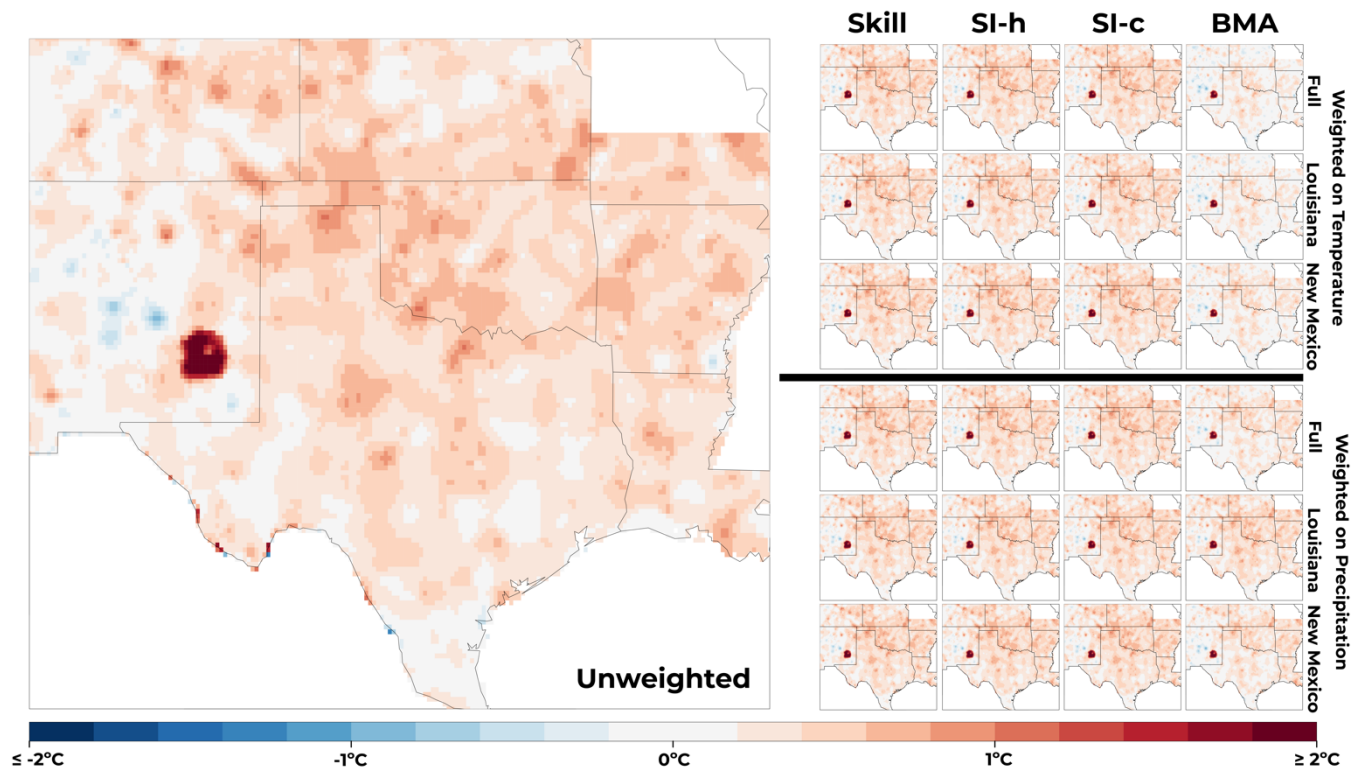
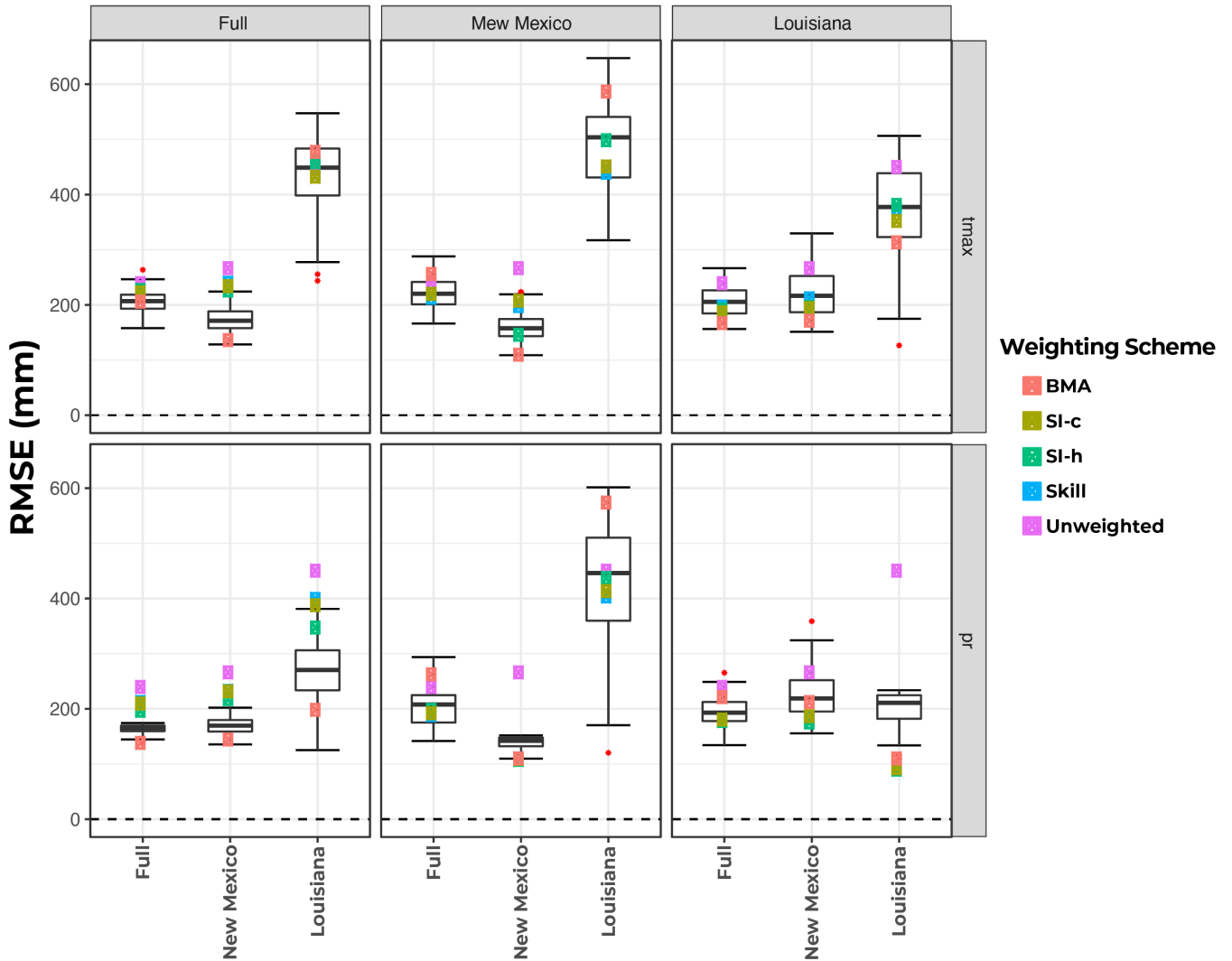


Figure S2: Same as Figure S1, but for the bias of ensemble mean high temperature of the LOCA ensemble.

CMIP5 Ensemble Mean RMSE - Precipitation



315

Figure S3: Historical RMSE using all 48 weighting schemes, applied to precipitation (pr) to all three domains for the CMIP5 ensemble. The top row is the results from weighting schemes derived with tmax, and the bottom row is the results from weighting schemes derived with pr. The left column is the results for weighting derived using the full domain, the middle column is the results for weighting derived using the New Mexico domain, and the right column is the results for weighting derived using the Louisiana. Within a given domain and variable, the results are shown from left to right for the domain the weights are applied to. The boxplots are the results from the 100 BMA posterior weights, with red dots used to represent outliers.

320

LOCA Ensemble Mean RMSE - Precipitation

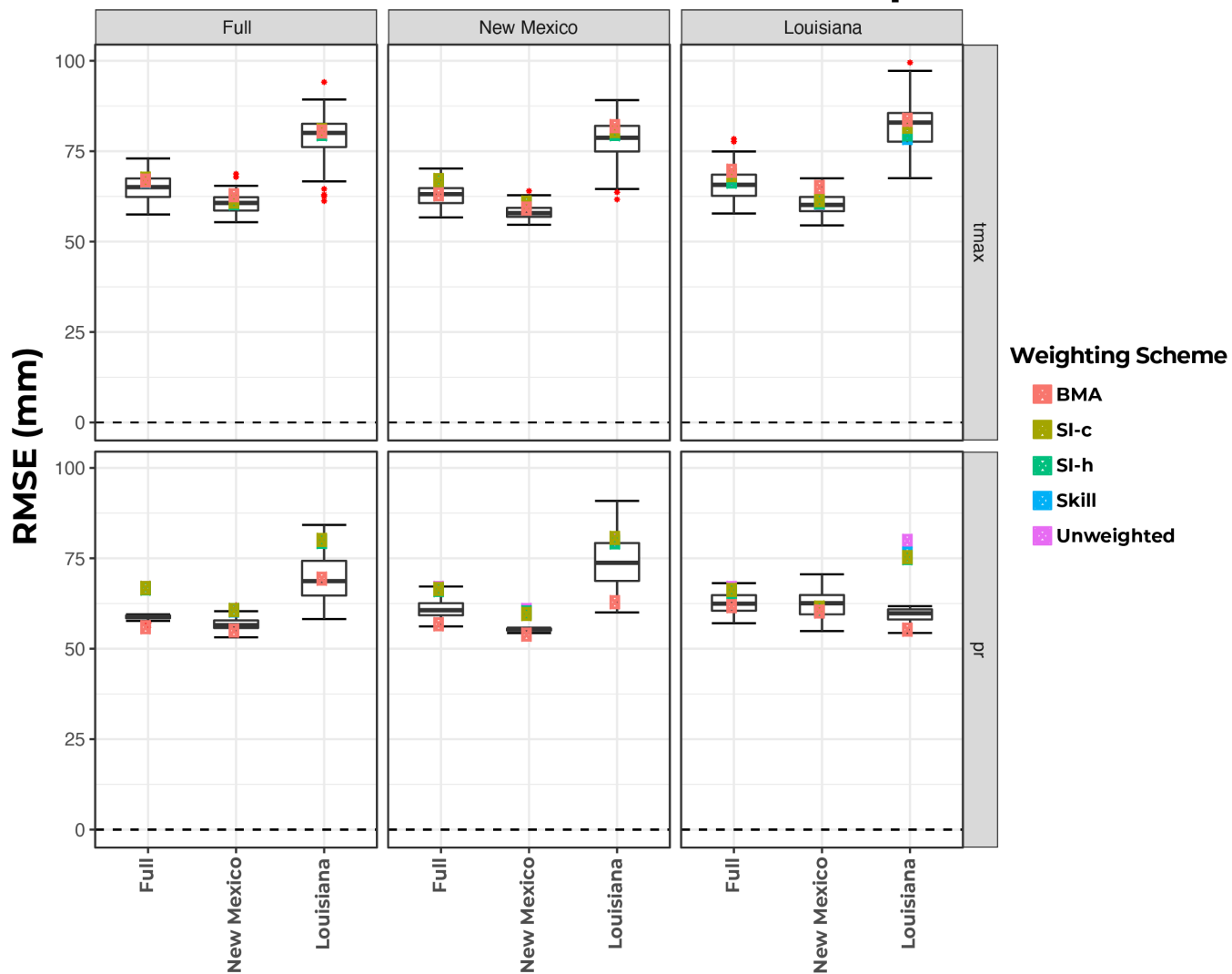


Figure S4: Same as Figure S3 for the LOCA ensemble precipitation.

325

CMIP5 Ensemble Mean RMSE - High Temperature

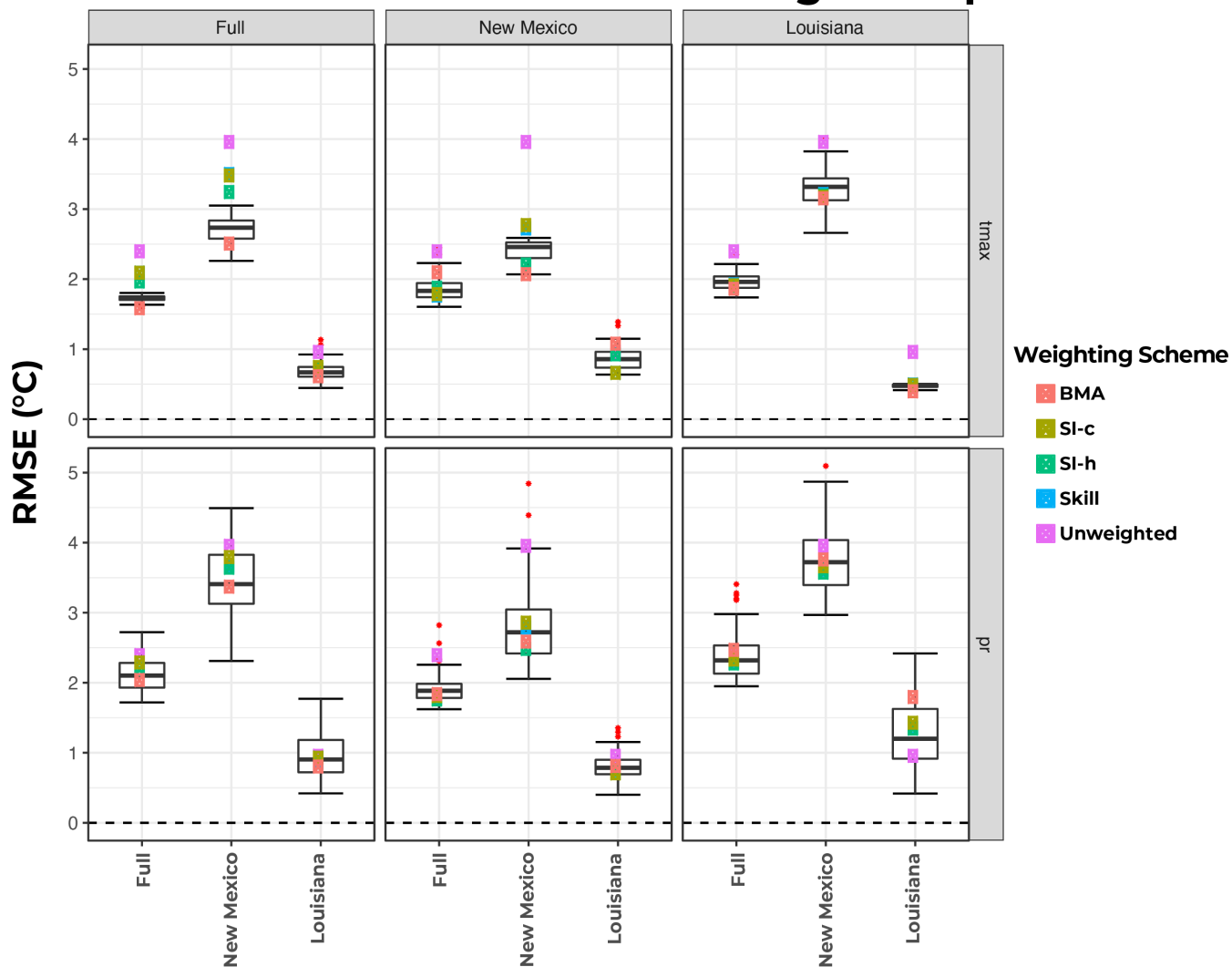
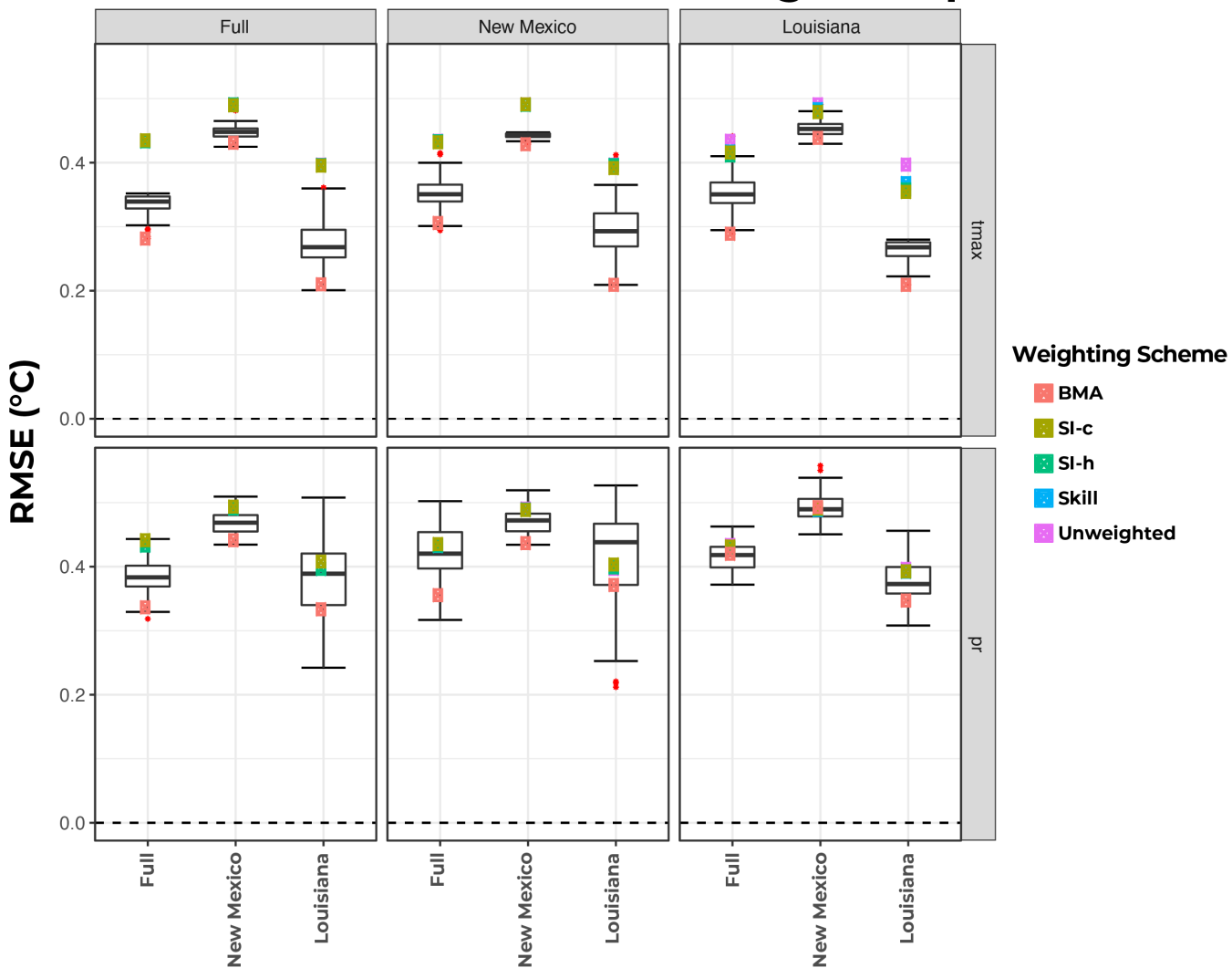


Figure S5: Historical RMSE using all 48 weighting schemes, applied to high temperature (tmax) to all three domains for the CMIP5 ensemble. The top row is the results from weighting schemes derived with tmax, and the bottom row is the results from weighting schemes derived with pr. The left column is the results for weighting derived using the full domain, the middle column is the results for weighting derived using the New Mexico domain, and the right column is the results for weighting derived using the Louisiana. Within a given domain and variable, the results are shown from left to right for the domain the weights are applied to. The boxplots are the results from the 100 BMA posterior weights, with red dots used to represent outliers.

330

LOCA Ensemble Mean RMSE - High Temperature



335 Figure S6: Same as Figure S5 for the LOCA ensemble high temperature.

340

345

350 **Table S1.** Global Climate Models used to create both the CMIP5 and LOCA ensembles (adopted from Wootten et al. 2020a).

Modeling Center or Group	Institute ID	Model Name
Commonwealth Scientific and Industrial Research Organization (CSIRO) and Bureau of Meteorology (BOM), Australia	CSIRO-BOM	ACCESS1-0
		ACCESS1-3
Beijing Climate Center, China Meteorological Administration	BCC	bcc-csm1-1-m
Canadian Centre for Climate Modelling and Analysis	CCCMA	CanESM2
National Center for Atmospheric Research	NCAR	CCSM4
Community Earth System Model Contributors	NSF-DOE-NCAR	CESM1-BGC
		CESM1-CAM5
Centro Euro-Mediterraneo per I Cambiamenti Climatici	CMCC	CMCC-CM
		CMCC-CMS
Commonwealth Scientific and Industrial Research Organization in collaboration with Queensland Climate Change Centre of Excellence	CSIRO-QCCCE	CSIRO-Mk3-6-0
EC-EARTH consortium	EC-EARTH	EC-EARTH
LASG, Institute of Atmospheric Physics, Chinese Academy of Sciences and CESS, Tsinghua University	LASG-CESS	FGOALS-g2
NOAA Geophysical Fluid Dynamics Laboratory	NOAA GFDL	GFDL-CM3
		GFDL-ESM2G
		GFDL-ESM2M
NASA Goddard Institute for Space Studies	NASS GISS	GISS-E2-H
		GISS-E2-R
Institut Pierre-Simon Laplace	IPSL	IPSL-CM5A-LR
		IPSL-CM5A-MR
Atmosphere and Ocean Research Institute (The University of Tokyo), National Institute for Environmental Studies, and Japan Agency for Marine-Earth Science and Technology	MIROC	MIROC5

Japan Agency for Marine-Earth Science and Technology, Atmosphere and Ocean Institute (The University of Tokyo), and National Institute for Environmental Studies	MIROC	MIROC-ESM-CHEM
		MIROC-ESM
Max Planck Institute for Meteorology	MPI-M	MPI-ESM-LR
		MPI-ESM-MR
Meteorological Research Institute	MRI	MRI-CGCM3
Norwegian Climate Centre	NCC	NorESM1-M

355

360

365

370

375

Table S2. Weights given to each model in the CMIP5 ensemble derived with the full domain.

Variable	GCM	Weighting scheme			
		Skill	SI-h	SI-c	BMA
tasmax	ACCESS1-0	0.05644228	0.04514523	0.07074581	0.11363804
	ACCESS1-3	0.04803347	0.05009975	0.02757792	1.52E-08

	bcc-csm1-1-m	0.05038122	0.04097768	0.0312682	0.02627195
	CanESM2	0.03312554	0.12162953	0.03424021	0.0734613
	CCSM4	0.04616865	0.0337523	0.02425615	0.0013554
	CESM1-BGC	0.04494195	0.03332879	0.02118354	4.50E-08
	CESM1-CAM5	0.04351808	0.03067799	0.03509343	1.59E-05
	CMCC-CM	0.05208671	0.04248304	0.06851263	0.21464608
	CMCC-CMS	0.05416892	0.04566091	0.03869899	5.54E-09
	CSIRO-Mk3-6-0	0.0558371	0.05558022	0.07131232	0.31794803
	EC-EARTH	0.04151551	0.03199337	0.0418087	2.58E-05
	FGOALS-g2	0.01175242	0.01846582	0.01019995	0.00987428
	GFDL-CM3	0.01616687	0.01859855	0.02192631	8.85E-06
	GFDL-ESM2G	0.01341388	0.01749179	0.00792139	2.58E-09
	GFDL-ESM2M	0.01576513	0.01848859	0.01522095	8.97E-12
	GISS-E2-H	0.03919189	0.03129483	0.03664499	0.00235282
	GISS-E2-R	0.03484401	0.03125194	0.0511487	3.42E-06
	IPSL-CM5A-LR	0.02305224	0.02230279	0.03212302	5.31E-09
	IPSL-CM5A-MR	0.03739726	0.02921484	0.05088791	9.11E-09
	MIROC5	0.0525348	0.04913526	0.0641872	1.47E-08
	MIROC-ESM-CHEM	0.04014272	0.05216315	0.05493447	0.0024138
	MIROC-ESM	0.03957272	0.05272626	0.05402526	5.26E-09
	MPI-ESM-LR	0.05077877	0.03756599	0.04265972	3.72E-07
	MPI-ESM-MR	0.05197698	0.04193178	0.04176602	0.23769678
	MRI-CGCM3	0.01952717	0.02120907	0.02865105	0.00019355
	NorESM1-M	0.02766371	0.02683054	0.02300515	9.35E-05
pr	ACCESS1-0	0.06045531	0.06070165	0.08307592	0.0072574
	ACCESS1-3	0.05917048	0.11086654	0.05877136	0.36569981
	bcc-csm1-1-m	0.03434178	0.03456922	0.03210624	4.25E-13
	CanESM2	0.04012332	0.04531193	0.02732204	6.18E-13
	CCSM4	0.03560204	0.0229925	0.02513995	4.49E-13
	CESM1-BGC	0.03413256	0.02305947	0.02267914	0.03404851
	CESM1-CAM5	0.03215632	0.02144499	0.02555282	2.94E-16
	CMCC-CM	0.06336952	0.0549192	0.0855987	0.19762237
	CMCC-CMS	0.05111864	0.03916385	0.04457927	0.02658297
	CSIRO-Mk3-6-0	0.04313327	0.03967106	0.0310102	0.02683317
	EC-EARTH	0.07558573	0.08196882	0.06257095	0.22716385

FGOALS-g2	0.02824788	0.01996533	0.03655295	0.00022352
GFDL-CM3	0.01929313	0.02456224	0.02274811	2.18E-07
GFDL-ESM2G	0.02120832	0.01712085	0.0193851	2.34E-10
GFDL-ESM2M	0.02809155	0.01920732	0.03652836	0.00080124
GISS-E2-H	0.04060163	0.04921506	0.05300536	2.80E-13
GISS-E2-R	0.0425454	0.08016262	0.04268746	0.00409878
IPSL-CM5A-LR	0.03070306	0.02757702	0.03884151	4.70E-07
IPSL-CM5A-MR	0.02603609	0.03986775	0.03429029	0.03726354
MIROC5	0.04701144	0.02917528	0.04639643	0.00165118
MIROC-ESM-CHEM	0.0233395	0.01905945	0.01679738	1.27E-07
MIROC-ESM	0.02096021	0.01792438	0.01353104	0.00027861
MPI-ESM-LR	0.0471387	0.03412552	0.04803859	0.02352033
MPI-ESM-MR	0.04650432	0.03567428	0.03924693	0.01155125
MRI-CGCM3	0.03245887	0.03503426	0.03764754	0.03539936
NorESM1-M	0.01667091	0.0166594	0.01589636	3.31E-06

380

385

390

Table S3. Weights given to each model in the CMIP5 ensemble derived with the Louisiana domain

Variable	GCM	Weighting Scheme			
		Skill	SI-h	SI-c	BMA
tasmax	ACCESS1-0	0.09539147	0.070859782	0.149472303	0.002577634
	ACCESS1-3	0.174880947	0.181461856	0.192657216	0.27621102
	bcc-csm1-1-m	0.043355531	0.06547964	0.029101179	0.11705057
	CanESM2	0.000143552	0.000363158	9.41E-05	2.90E-06
	CCSM4	0.084536835	0.062718253	0.044171395	0.003062876

	CESM1-BGC	0.089093012	0.062157894	0.044244131	7.03E-05
	CESM1-CAM5	0.058618953	0.05146394	0.066439396	0.000333261
	CMCC-CM	0.0460721	0.093738585	0.050348496	0.30202615
	CMCC-CMS	0.142652184	0.110288875	0.115395471	4.17E-06
	CSIRO-Mk3-6-0	0.032059914	0.036493165	0.023989689	7.11E-08
	EC-EARTH	2.67E-05	7.18E-05	3.18E-05	1.11E-11
	FGOALS-g2	5.97E-11	1.25E-10	1.04E-10	1.26E-20
	GFDL-CM3	9.08E-10	9.11E-10	1.83E-09	0.001832793
	GFDL-ESM2G	5.25E-12	8.78E-12	2.99E-12	0.000254789
	GFDL-ESM2M	6.98E-10	7.83E-10	4.64E-10	1.03E-09
	GISS-E2-H	0.000185671	0.000512926	0.000343065	1.55E-05
	GISS-E2-R	1.45E-09	1.69E-09	2.17E-09	0.032775603
	IPSL-CM5A-LR	0.002876298	0.004814258	0.003355854	0.06681373
	IPSL-CM5A-MR	0.04559663	0.047372655	0.070531696	2.05E-05
	MIROC5	0.001899871	0.006186466	0.002876237	0.19016249
	MIROC-ESM-CHEM	0.000376663	0.000723095	0.000812865	0.00563014
	MIROC-ESM	0.002539795	0.004909342	0.003857348	0.000476253
	MPI-ESM-LR	0.101817678	0.07301403	0.125881564	0.000218828
	MPI-ESM-MR	0.076691645	0.125396124	0.075192409	0.000460369
	MRI-CGCM3	1.02E-09	1.32E-09	1.55E-09	6.45E-15
	NorESM1-M	0.001184554	0.001974168	0.001203786	1.12E-09
	ACCESS1-0	0.094507226	0.083513755	0.097392677	2.64E-06
	ACCESS1-3	0.334341954	0.356209181	0.299044271	0.26946759
	bcc-csm1-1-m	9.22E-09	4.05E-09	9.82E-09	0.014008402
	CanESM2	2.13E-10	8.63E-11	2.18E-10	0.000247708
	CCSM4	3.35E-06	8.54E-07	2.43E-06	1.55E-06
	CESM1-BGC	9.76E-07	2.49E-07	7.39E-07	6.72E-05
	CESM1-CAM5	8.32E-07	2.63E-07	6.41E-07	7.62E-10
pr	CMCC-CM	8.72E-05	3.72E-05	8.62E-05	0.009259525
	CMCC-CMS	3.21E-05	1.07E-05	2.27E-05	4.27E-08
	CSIRO-Mk3-6-0	8.16E-08	2.39E-08	8.65E-08	0.000262672
	EC-EARTH	0.192570184	0.200112652	0.203466603	3.20E-10
	FGOALS-g2	2.03E-08	5.29E-09	2.17E-08	7.59E-18
	GFDL-CM3	3.36E-05	1.25E-05	2.56E-05	6.11E-05
	GFDL-ESM2G	3.18E-13	1.79E-13	2.60E-13	0.000759058

GFDL-ESM2M	2.84E-09	8.85E-10	3.04E-09	0.006637048
GISS-E2-H	0.058676084	0.040063901	0.062791018	4.98E-05
GISS-E2-R	0.267327869	0.285087916	0.286076502	0.65528678
IPSL-CM5A-LR	6.72E-12	2.49E-12	7.06E-12	2.83E-07
IPSL-CM5A-MR	3.65E-10	1.51E-10	3.91E-10	0.000154533
MIROC5	2.51E-05	9.81E-06	2.03E-05	5.23E-15
MIROC-ESM-CHEM	4.86E-12	1.65E-12	3.86E-12	0.026742395
MIROC-ESM	3.65E-12	1.24E-12	2.96E-12	9.68E-07
MPI-ESM-LR	3.91E-07	9.63E-08	4.11E-07	0.00039702
MPI-ESM-MR	2.12E-08	5.68E-09	2.22E-08	0.016593524
MRI-CGCM3	0.052393055	0.034940792	0.051069782	2.19E-07
NorESM1-M	1.31E-09	4.56E-10	1.37E-09	2.07E-11

395

400

405

Table S4. Weights given to each model in the CMIP5 ensemble derived with the New Mexico domain

Variable	GCM	Weighting Scheme			BMA
		Skill	SI-h	SI-c	
tasmax	ACCESS1-0	0.09939927	0.06984359	0.08756062	8.71E-05
	ACCESS1-3	0.07152743	0.05473646	0.04899342	1.00E-08
	bcc-csm1-1-m	0.05457664	0.02628373	0.03998063	0.02751101
	CanESM2	0.10754797	0.35175889	0.08728388	0.54658804
	CCSM4	0.02878184	0.0142128	0.02663433	0.00036638
	CESM1-BGC	0.02671602	0.01335277	0.01805697	2.20E-05
	CESM1-CAM5	0.02426858	0.01269948	0.02924927	6.75E-06
	CMCC-CM	0.05521459	0.03162108	0.06875559	2.92E-05

CMCC-CMS	0.06509256	0.03665949	0.0655887	0.00654376
CSIRO-Mk3-6-0	0.10633306	0.15640465	0.11542768	0.29138712
EC-EARTH	0.01702482	0.00965101	0.01974289	0.02184139
FGOALS-g2	0.00119852	0.00108409	0.00125317	0.00444444
GFDL-CM3	0.00125992	0.00100038	0.00159064	0.01005276
GFDL-ESM2G	0.00029932	0.0003652	0.00034635	0.00801717
GFDL-ESM2M	0.00061458	0.00062267	0.00073893	0.0013548
GISS-E2-H	0.01778507	0.0095029	0.02026868	0.00536214
GISS-E2-R	0.01855788	0.00994391	0.02342929	1.41E-05
IPSL-CM5A-LR	0.00163974	0.00131537	0.00207017	0.05934004
IPSL-CM5A-MR	0.00770011	0.00479588	0.00972135	1.53E-13
MIROC5	0.07250547	0.04730678	0.08723717	0.00020178
MIROC-ESM-CHEM	0.06188476	0.04569864	0.07812881	0.00855385
MIROC-ESM	0.06106126	0.04733796	0.07708915	5.06E-08
MPI-ESM-LR	0.03994754	0.01966853	0.0423591	1.47E-21
MPI-ESM-MR	0.05044133	0.0260291	0.03826585	0.00788137
MRI-CGCM3	0.00160389	0.00146294	0.00202491	0.00039472
NorESM1-M	0.00701784	0.00664171	0.00820246	8.92E-09
ACCESS1-0	0.00742511	0.00977952	0.00862007	0.01409884
ACCESS1-3	0.18535919	0.16072249	0.17455917	0.00463789
bcc-csm1-1-m	0.00462169	0.00388373	0.00420513	8.42E-07
CanESM2	0.22271141	0.30465671	0.23385789	0.34198563
CCSM4	8.17E-10	4.14E-10	5.93E-10	0.00255201
CESM1-BGC	4.22E-10	2.22E-10	4.54E-10	0.0006526
CESM1-CAM5	6.93E-10	5.38E-10	5.80E-10	8.16E-07
CMCC-CM	0.07676102	0.0762634	0.08911065	0.04955513
CMCC-CMS	0.00390915	0.00257245	0.00248165	3.78E-08
CSIRO-Mk3-6-0	0.13373349	0.16496307	0.09658888	0.22161446
EC-EARTH	0.13123493	0.09037766	0.12697972	1.36E-11
FGOALS-g2	5.86E-07	4.17E-07	5.23E-07	1.00E-09
GFDL-CM3	2.99E-13	3.32E-13	3.44E-13	0.02764009
GFDL-ESM2G	7.78E-13	1.04E-12	7.71E-13	0.00162559
GFDL-ESM2M	1.42E-08	9.28E-09	1.39E-08	0.00035877
GISS-E2-H	2.35E-06	2.42E-06	2.72E-06	0.00429871
GISS-E2-R	0.00019241	0.00021432	0.00018154	0.00103039

pr

IPSL-CM5A-LR	0.00505714	0.00519675	0.00585064	6.66E-11
IPSL-CM5A-MR	0.20511241	0.16280282	0.23729592	0.32307108
MIROC5	3.12E-05	3.46E-05	2.03E-05	2.50E-07
MIROC-ESM-CHEM	3.02E-07	1.94E-07	2.76E-07	4.63E-10
MIROC-ESM	2.35E-09	1.52E-09	2.03E-09	0.00203139
MPI-ESM-LR	0.00162742	0.00117823	0.0017721	0.00059298
MPI-ESM-MR	0.02222018	0.01735118	0.01847282	0.00049619
MRI-CGCM3	2.82E-12	3.48E-12	3.28E-12	0.00375236
NorESM1-M	4.77E-16	5.77E-16	5.20E-16	3.94E-06

410

415

420

425 Table S5. Weights given to each model in the LOCA ensemble derived with the full domain.

Variable	GCM	Weighting Scheme			
		Skill	SI-h	SI-c	BMA
tasmax	ACCESS1-0	0.03843002	0.03835969	0.04590839	0.00685415
	ACCESS1-3	0.03845163	0.03840102	0.0230868	0.01370196
	bcc-csm1-1-m	0.03855926	0.03845582	0.02400497	5.50E-09
	CanESM2	0.03867074	0.03863661	0.03850615	0.12487015
	CCSM4	0.03861473	0.0385269	0.02006005	1.08E-05
	CESM1-BGC	0.03868285	0.03866551	0.01842328	0.00799637
	CESM1-CAM5	0.03843966	0.03836553	0.03280679	2.86E-06
	CMCC-CM	0.03831829	0.03826985	0.04709167	0.00275627
	CMCC-CMS	0.0384972	0.03834852	0.02591459	0.00313127
	CSIRO-Mk3-6-0	0.03856268	0.03844201	0.047086	0.0076736
	EC-EARTH	0.03818016	0.03821145	0.03660173	0.00062814

FGOALS-g2	0.03811864	0.03818104	0.04899749	0.01718842
GFDL-CM3	0.03858206	0.03846847	0.05081382	1.82E-05
GFDL-ESM2G	0.03831407	0.03836043	0.02429695	1.38E-11
GFDL-ESM2M	0.03848291	0.03845213	0.0353421	0.00121971
GISS-E2-H	0.03867795	0.03864678	0.03338944	1.02E-12
GISS-E2-R	0.03851628	0.03842569	0.05367807	0.00190605
IPSL-CM5A-LR	0.03753834	0.03824003	0.05010429	1.95E-10
IPSL-CM5A-MR	0.0385945	0.03846255	0.0511938	5.04E-07
MIROC5	0.03832068	0.03826415	0.04551554	0.00049982
MIROC-ESM-CHEM	0.03847912	0.03841837	0.05095552	0.00447711
MIROC-ESM	0.03878386	0.0391118	0.05113012	0.00068839
MPI-ESM-LR	0.03829208	0.03825354	0.03208248	9.01E-09
MPI-ESM-MR	0.03843451	0.03832186	0.02608251	1.03E-08
MRI-CGCM3	0.03884306	0.03920701	0.05403101	0.8063758
NorESM1-M	0.03861473	0.03850324	0.03289646	4.28E-07
ACCESS1-0	0.03868751	0.03845149	0.05538722	0.05701355
ACCESS1-3	0.03748008	0.03779315	0.02881096	5.15E-06
bcc-csm1-1-m	0.0385428	0.03826234	0.03502586	1.28E-08
CanESM2	0.03914891	0.04019539	0.04869883	0.26372065
CCSM4	0.03910103	0.03907033	0.02509709	0.07630813
CESM1-BGC	0.03915312	0.0393793	0.0245094	0.23863091
CESM1-CAM5	0.03866983	0.03830047	0.02880474	0.00185555
CMCC-CM	0.03888981	0.03873128	0.05428339	0.00045197
CMCC-CMS	0.03820094	0.03791453	0.02723303	3.79E-05
CSIRO-Mk3-6-0	0.03815281	0.03785883	0.03146579	1.01E-05
EC-EARTH	0.03786059	0.03800275	0.03116372	0.00077738
FGOALS-g2	0.03810924	0.03791663	0.0491427	0.00126907
GFDL-CM3	0.03865299	0.03829648	0.03417903	0.01501184
GFDL-ESM2G	0.03836649	0.03855796	0.03071856	0.00195493
GFDL-ESM2M	0.03860002	0.0390896	0.04583803	0.00049713
GISS-E2-H	0.03802192	0.03791928	0.04198333	2.87E-08
GISS-E2-R	0.03860631	0.03907614	0.03709764	0.01370005
IPSL-CM5A-LR	0.0377017	0.03784103	0.05264404	5.79E-14
IPSL-CM5A-MR	0.03853391	0.03821201	0.05619112	0.0001892
MIROC5	0.03794169	0.03774639	0.03259612	0.00032932

pr

	MIROC-ESM-CHEM	0.03728185	0.03796482	0.04529474	0.00035278
	MIROC-ESM	0.03913399	0.0394354	0.0387394	0.32416294
	MPI-ESM-LR	0.03892274	0.03867247	0.04292192	4.61E-11
	MPI-ESM-MR	0.03879659	0.0384649	0.0408521	3.17E-05
	MRI-CGCM3	0.03853771	0.03816694	0.03334386	0.00367149
	NorESM1-M	0.03890546	0.0386801	0.02797739	1.82E-05

430

435

440

445

450

455

460

Table S6. Weights given to each model in the LOCA ensemble derived with the Louisiana domain.

Variable	GCM	Weighting Scheme			
		Skill	SI-h	SI-c	BMA
tasmax	ACCESS1-0	0.03100221	0.02915454	0.040746	6.71E-07
	ACCESS1-3	0.05040064	0.05260764	0.04667151	9.12E-05
	bcc-csm1-1-m	0.04453285	0.04020767	0.03045576	0.00119831
	CanESM2	0.0324218	0.0305315	0.02037736	4.78E-08
	CCSM4	0.04409604	0.03989712	0.01897782	2.84E-06
	CESM1-BGC	0.03866978	0.03390751	0.01748584	2.28E-11
	CESM1-CAM5	0.03803129	0.03346863	0.03574216	0.00037567
	CMCC-CM	0.03195021	0.02961334	0.0283389	3.16E-07
	CMCC-CMS	0.0405695	0.03587539	0.02897122	2.05E-14
	CSIRO-Mk3-6-0	0.03478198	0.03111926	0.0192973	0.03749378
	EC-EARTH	0.0408683	0.03668547	0.0388582	0.00026337
	FGOALS-g2	0.03158036	0.02978617	0.04310589	0.01539686
	GFDL-CM3	0.04461578	0.04045792	0.07244148	0.007909
	GFDL-ESM2G	0.02658537	0.0276331	0.0123474	0.00743341
	GFDL-ESM2M	0.04360985	0.03935089	0.02266463	0.07300591
	GISS-E2-H	0.04184729	0.03719441	0.05484493	0.08217037
	GISS-E2-R	0.0438759	0.04043294	0.06083922	3.42E-09
	IPSL-CM5A-LR	0.01431324	0.02627194	0.0149504	0.00096226
	IPSL-CM5A-MR	0.03787995	0.03322969	0.0464877	5.01E-08
	MIROC5	0.03040706	0.02878095	0.0325194	0.00615986
	MIROC-ESM-CHEM	0.04739619	0.04669298	0.09542163	1.12E-05
	MIROC-ESM	0.05351149	0.0837266	0.06049142	2.27E-08
	MPI-ESM-LR	0.02554219	0.02738016	0.02248943	7.49E-09
	MPI-ESM-MR	0.0382573	0.03348629	0.03069654	2.74E-05
MRI-CGCM3	0.05464586	0.07874774	0.07465364	0.76382034	
NorESM1-M	0.03860759	0.03376014	0.03012423	0.00367713	
pr	ACCESS1-0	0.03428467	0.03337926	0.0471579	3.59E-06
	ACCESS1-3	0.03500028	0.0319283	0.02168169	0.00099018
	bcc-csm1-1-m	0.04200078	0.04145073	0.04089891	3.25E-06
	CanESM2	0.04731829	0.06025351	0.03845356	0.00324284
	CCSM4	0.04888984	0.05478434	0.02866901	0.52941953
	CESM1-BGC	0.03951288	0.03666173	0.023805	2.86E-09

CESM1-CAM5	0.04484676	0.04309665	0.03032724	1.69E-05
CMCC-CM	0.03920264	0.03482159	0.03422899	0.00088496
CMCC-CMS	0.03455911	0.03127403	0.02087831	2.59E-10
CSIRO-Mk3-6-0	0.03392731	0.03150069	0.03880255	1.97E-05
EC-EARTH	0.03734051	0.03616185	0.02463845	0.10341634
FGOALS-g2	0.03853889	0.03398473	0.06759691	4.65E-06
GFDL-CM3	0.03719562	0.03269489	0.03002907	0.00052307
GFDL-ESM2G	0.02532499	0.03088774	0.0190383	4.94E-05
GFDL-ESM2M	0.04803501	0.05030028	0.05839608	7.02E-08
GISS-E2-H	0.03598987	0.03185216	0.05534456	6.34E-14
GISS-E2-R	0.04885113	0.06943518	0.09182185	0.30134026
IPSL-CM5A-LR	0.02606843	0.03087662	0.02707114	0.01675307
IPSL-CM5A-MR	0.03918806	0.03495953	0.06841608	0.02997501
MIROC5	0.03332045	0.03072366	0.02642121	0.00620631
MIROC-ESM-CHEM	0.02447897	0.03103161	0.02652211	4.62E-13
MIROC-ESM	0.03892406	0.0349099	0.04565354	0.00676324
MPI-ESM-LR	0.04413614	0.03954262	0.02848804	0.00030145
MPI-ESM-MR	0.04367644	0.04051209	0.05028874	1.03E-08
MRI-CGCM3	0.03804345	0.03690593	0.02468679	5.44E-18
NorESM1-M	0.04134546	0.03607037	0.03068398	8.62E-05

465

470

475

480 Table S7. Weights given to each model in the LOCA ensemble derived with the New Mexico domain.

Variable	GCM	Weighting Scheme			
		Skill	SI-h	SI-c	BMA
tasmax	ACCESS1-0	0.038672887	0.038579983	0.03426941	0.00541779
	ACCESS1-3	0.038599333	0.038590107	0.02498509	0.00034678
	bcc-csm1-1-m	0.038436478	0.038275525	0.02764994	7.30E-09
	CanESM2	0.038736479	0.038860415	0.02559203	0.00529255
	CCSM4	0.038560894	0.03846669	0.03527624	1.96E-05
	CESM1-BGC	0.038514472	0.038402329	0.02623952	0.00786877
	CESM1-CAM5	0.038760384	0.038747631	0.03708614	2.45E-14
	CMCC-CM	0.038291854	0.038233855	0.04326728	2.71E-05
	CMCC-CMS	0.038562448	0.038367172	0.03360558	0.01306485
	CSIRO-Mk3-6-0	0.038597425	0.038447408	0.02981096	0.00236676
	EC-EARTH	0.038235708	0.038183425	0.03791847	0.01591943
	FGOALS-g2	0.038319082	0.038195221	0.02640804	0.10740954
	GFDL-CM3	0.038572509	0.038443596	0.04979786	0.01498851
	GFDL-ESM2G	0.037892374	0.038199002	0.04289486	0.00120082
	GFDL-ESM2M	0.037941002	0.038069604	0.04354575	0.00034764
	GISS-E2-H	0.038765416	0.038748946	0.03984545	0.00071154
	GISS-E2-R	0.038491206	0.038360979	0.04970111	3.00E-06
	IPSL-CM5A-LR	0.037694462	0.038141813	0.04866371	1.22E-07
	IPSL-CM5A-MR	0.038550197	0.03836664	0.0497601	1.48E-05
	MIROC5	0.038304444	0.038193684	0.03785574	0.00024818
	MIROC-ESM-CHEM	0.038355964	0.038455436	0.0495178	2.76E-06
	MIROC-ESM	0.038802399	0.039455382	0.05009398	0.39150229
	MPI-ESM-LR	0.03854897	0.038370109	0.03560064	4.36E-08
	MPI-ESM-MR	0.038260687	0.038178584	0.0272849	0.01969286
MRI-CGCM3	0.038829456	0.039091302	0.05013787	0.41355423	
NorESM1-M	0.03870347	0.038575163	0.04319152	6.76E-09	
pr	ACCESS1-0	0.042228086	0.041620052	0.05132523	0.00011028
	ACCESS1-3	0.035909539	0.0358652	0.03924984	1.78E-09
	bcc-csm1-1-m	0.038770311	0.037541673	0.03977957	0.01118545
	CanESM2	0.043546667	0.044854048	0.05296066	0.54977095
	CCSM4	0.040897988	0.040825631	0.02987004	7.78E-06
	CESM1-BGC	0.040276913	0.039221399	0.02640718	1.02E-08

CESM1-CAM5	0.039455422	0.037872859	0.0278062	0.04866509
CMCC-CM	0.042878762	0.042500047	0.0515471	0.00156692
CMCC-CMS	0.039816723	0.038480566	0.04326805	0.02204018
CSIRO-Mk3-6-0	0.033712335	0.033900471	0.02659054	3.27E-05
EC-EARTH	0.041145403	0.040675815	0.0443557	0.06073666
FGOALS-g2	0.037283675	0.036121315	0.03434268	0.00021219
GFDL-CM3	0.041875714	0.041035937	0.04063304	0.00364462
GFDL-ESM2G	0.040770072	0.039451366	0.03809098	0.00012032
GFDL-ESM2M	0.028065942	0.033041085	0.02683618	9.66E-07
GISS-E2-H	0.038398352	0.037218574	0.04660775	0.00208044
GISS-E2-R	0.034001738	0.03428959	0.02272487	0.00038251
IPSL-CM5A-LR	0.036190882	0.03680316	0.04402027	7.16E-15
IPSL-CM5A-MR	0.040312614	0.038755043	0.0490344	2.31E-13
MIROC5	0.032409579	0.033285867	0.02816095	1.30E-13
MIROC-ESM-CHEM	0.030363131	0.032907731	0.02966293	9.21E-06
MIROC-ESM	0.043440225	0.043740774	0.04442732	0.26837324
MPI-ESM-LR	0.043939628	0.046936707	0.05282253	0.01981132
MPI-ESM-MR	0.035504772	0.035278711	0.03439191	0.00443399
MRI-CGCM3	0.036457875	0.035892539	0.03832491	0.00014555
NorESM1-M	0.042347654	0.04188384	0.03675919	0.00666958